Review of Scientific Instruments ARTICLE pubs.aip.org/aip/rsi

Experimental implementation of an ion-nanowire hybrid system

Cite as: Rev. Sci. Instrum. 96, 063203 (2025); doi: 10.1063/5.0260410
Submitted: 24 January 2025 • Accepted: 3 June 2025 •
Published Online: 18 June 2025

M. Weegen,[1,2] P. N. Fountas,[1,2] M. Poggio,[3,2,a)] and S. Willitsch[1,2,b)]

AFFILIATIONS

[1] Department of Chemistry, University of Basel, Klingelbergstrasse 80, 4056 Basel, Switzerland
[2] Swiss Nanoscience Institute, Klingelbergstrasse 82, 4056 Basel, Switzerland
[3] Department of Physics, University of Basel, Klingelbergstrasse 82, 4056 Basel, Switzerland

[a)] martino.poggio@unibas.ch
[b)] **Author to whom correspondence should be addressed:** stefan.willitsch@unibas.ch

ABSTRACT

Hybrid systems aim toward the combination of different types of physical platforms exhibiting complementary properties and advantages to develop new applications and technologies. In a recent publication [Weegen *et al.*, Phys. Rev. Lett. **133**, 223201 (2024)], we demonstrated a hybrid system consisting of two coupled oscillators: laser-cooled atomic Ca^+ ions confined in a miniaturized linear radio frequency trap and a charged Ag_2Ga nanowire. Here, we detail the design considerations and experimental implementation of the system and characterize the effect of the nanowire assembly on the trapping potential for ions using numerical simulations and experiments. Moreover, we further detail the resonant excitation of trapped ions by the mechanical drive of the nanowire.

I. INTRODUCTION

The development of hybrid systems has received considerable interest in recent years.[1–3] Experiments in this domain aim at coupling different physical platforms in order to exploit complementary advantages offered by the individual constituents for new applications, e.g., in the quantum technologies.[4] A variety of implementations ranging from neutral and charged atoms[5–7] and spins[8,9] coupled to solid-state systems such as quantum dots,[10] superconductors,[11] and nanomechanical oscillators[12,13] have been demonstrated over the past years.

One of the best-established, highly controllable quantum systems are trapped ions in linear radio frequency traps.[14] The developments in modern laser cooling and quantum-state engineering enabled the preparation of trapped atomic and molecular ions in their motional ground states, their coherent manipulation, and their application in quantum information.[15,16]

Ions confined in radio frequency traps behave similar to classical or quantum harmonic oscillators.[15] As such, coupling to other types of (mechanical) oscillators[5] such as nanowires, cantilevers, trapped nanoparticles, and nanomembranes offers the prospect to realize coupled oscillator systems[7,17,18] on the interface between atomic and solid state physics. Control over the subsystems offers prospects for bidirectional sympathetic cooling[19–22] for the manipulation and readout of motional quantum states,[23,24] for the sensing of forces,[25] and for the generation of tailored motional quantum states.[26]

In a previous publication,[27] we presented for the first time a hybrid system consisting of laser-cooled ions coupled to an oscillating nanowire. The ions were trapped in a miniaturized wafer radio frequency ion trap and coupled to a charged Ag_2Ga nanooscillator placed in the vicinity of the trap center.[26] The subsystems were coupled by their mutual Coulomb interaction. Using this setup, we demonstrated the resonant motional excitation of ions by mechanical oscillation of the nanowire in the classical regime and characterized the influence of salient experimental parameters such as mechanical drive strength, charge on the wire, and its distance from the ions on the dynamics of the ion excitation.

While our previous publications[26,27] discussed the theoretical description, experimental demonstration, and scientific perspectives of the present hybrid system, here we present the details of the implementation of this experiment. We describe the detailed design and

construction of the setup including the ion trap, nanowire integration, vacuum chamber, and optical setup. We detail the optical readout of the nanowire oscillation and the measurement of the driven ion motion. We characterize the effect of the nanowire on the trapping potential and motional frequencies of the ions as well as the mechanical excitation of the ion motion.

II. EXPERIMENTAL SETUP

A. Linear radio frequency wafer ion trap

The heart of the experimental setup consisted of a linear radio frequency ion trap for laser-cooled $^{40}Ca^{+}$ ions. The trap was fabricated from layered, laser-cut aluminum-oxide wafers of thickness $h = 200\ \mu$m stacked on a printed circuit board (PCB),[26] as shown in Fig. 1(a). The wafers were coated with gold to ensure electrical conductivity.

The assembly featured two pairs of diagonally opposed radio frequency (RF) and direct current (DC) electrode wafers [cross-sectional view in Fig. 1(c)] for the generation of a dynamic electric potential to trap the ions.[14] The sinusoidal RF trapping voltage at frequency $\Omega \approx 2\pi \times 21.6$ MHz was generated by an arbitrary waveform generator, amplified, and subsequently, connected to a helical resonator[28] before reaching the trap electrodes. The DC wafers were split into seven individually addressable segments with length

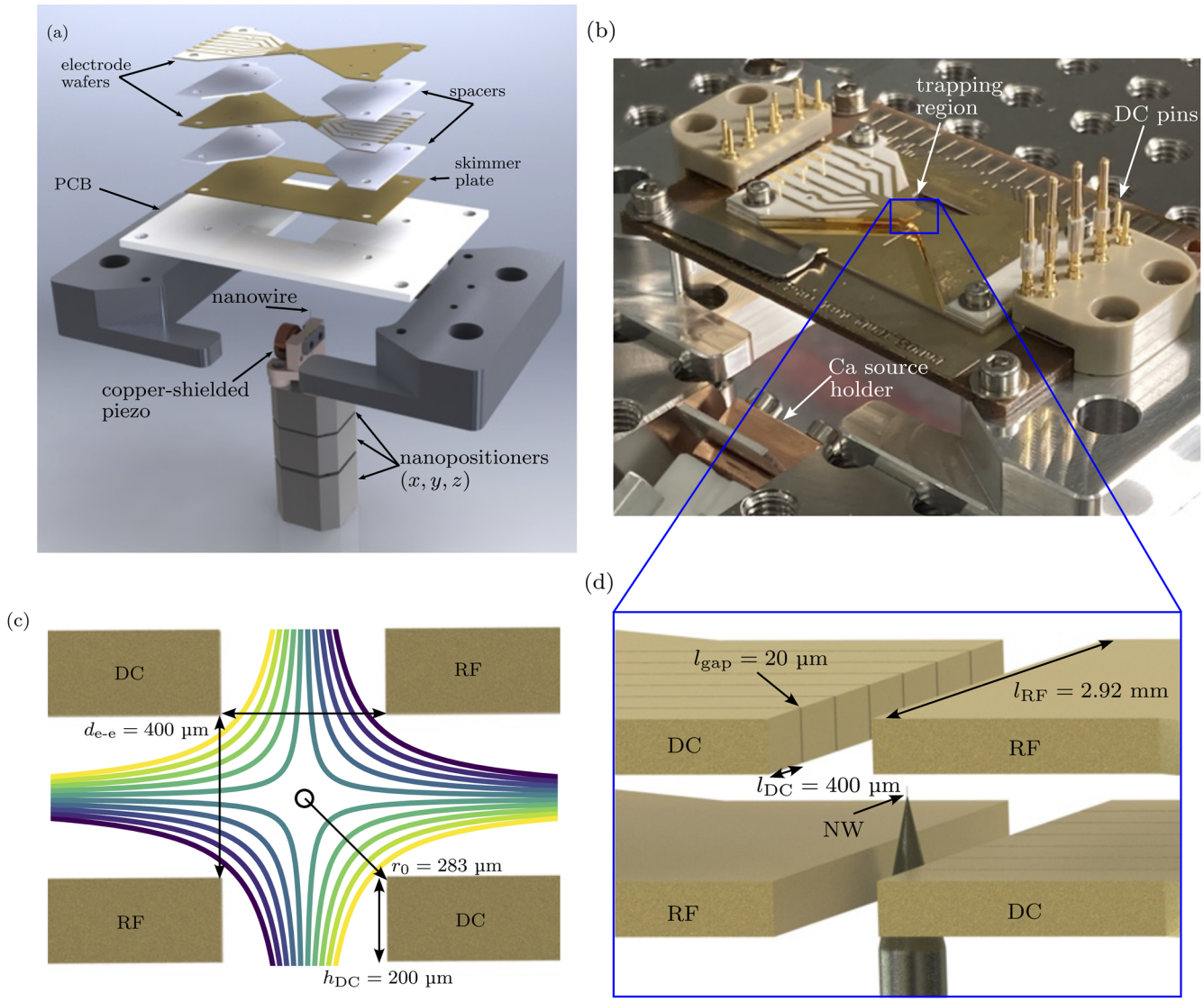

FIG. 1. (a) Exploded schematic of the wafer radio frequency ion trap used in the present experiments with nanowire-positioning assembly underneath. (b) Photograph of the assembled trap. (c) Cross section of the trap along the radial plane, with electrode dimensions indicated. Equipotential lines of the quadrupolar RF potential without the presence of the nanowire are also shown. (d) Schematic of the nanowire (NW) inserted into the trap. The DC electrodes were segmented into seven individually addressable electrodes.

l_{DC} = 400 μm separated by l_{gap} = 20 μm. This design enabled for the flexible shaping of the trapping potentials and the generation of multiple possible trapping regions by the application of appropriate static voltages to the individual segments.[26] The RF electrode wafers exhibited a length of l_{RF} = 2.92 mm spanning over the length of the DC electrodes. The electrode-to-electrode distance amounted to d_{ee} = 400 μm, as indicated in Fig. 1(c).

The DC electrode segments were wire-bonded to the underlying PCB and supplied with static voltages from a National Instruments PXIe-6739 digital-to-analog converter (DAC) card via spring-loaded pin connectors in contact with the respective PCB channel [Fig. 1(b)]. A low-pass filter with a cutoff frequency ω_{cut} = 1 Hz consisting of resistance R = 100 kΩ and capacitance C = 10 μF was added to each DC supply channel to suppress RF pickup. An additional electrode (not shown in Fig. 1) was mounted on top of the trap for the application of static compensation voltages and AC potentials for the resonant excitation of the ion motion.[29]

B. Nanowire assembly

The ion trap was interfaced with an electrically conducting Ag_2Ga nanowire (NaugaNeedles)[30] of length $l_{nw} \approx 16$ μm and diameter $d_{nw} \approx 150$ nm attached to the tip of a tungsten holder, as shown in Fig. 1(d). A static voltage applied to the nanowire ensured its electrostatic coupling to the trapped Ca^+ ions. The nanowire was mounted on a stack consisting of two attocube ANPx51 nanpositioners for horizontal placement and one attocube ANPz51 nanpositioner for vertical positioning thus enabling its placement at an arbitrary position within the trapping region. Figure 1(a) shows the nanowire positioning setup located below the ion trap. The tungsten holder with a length of $l_{holder} \approx 4.8$ mm was clamped to a PEEK (polyether ether ketone) mount. The assembly was mechanically driven with a piezo disk actuator of diameter d = 5 mm and thickness h = 2 mm clamped to the opposite side of the PEEK mount with firm mechanical contact. Applying an alternating current (AC) at frequency f_{drive} to the piezo disk mechanically excited the tungsten holder and the nanowire on its tip. A strong excitation of the nanowire was only achieved at drive frequencies f_{drive} close to a mechanical resonance frequency f_n of the assembly (see Sec. III A). The piezo actuator was encased in a grounded copper shield to prevent the penetration of the applied AC potential to the trapping region, which could result in spurious electrical excitation of the trapped ions.

C. Vacuum chamber and laser setup

A schematic of the experiment including the optical setup is shown in Fig. 2. The trap was housed in an octagon-shaped ultrahigh-vacuum chamber (Kimball Physics) featuring eight lateral CF40 flanges and a CF200 viewport on the top. Flanges 2, 4, 6, and 8 shown in Fig. 2 were used for feedthroughs of electrical connections to the trap electrodes, nanopositioners, and the piezo actuator. The remaining four flanges were fitted with viewports for optical access to the trap. Ultrahigh vacuum at pressures of order 10^{-9} mbar was maintained by a turbomolecular pump (Leybold Oerlikon MAG W600iP) assisted by a titanium sublimation pump (Agilent).

Calcium was evaporated toward the trap center by resistive heating of a getter source (AlfaVakuo), as depicted in Fig. 1(b). A skimmer of 1 mm diameter was installed in front of the oven nozzle

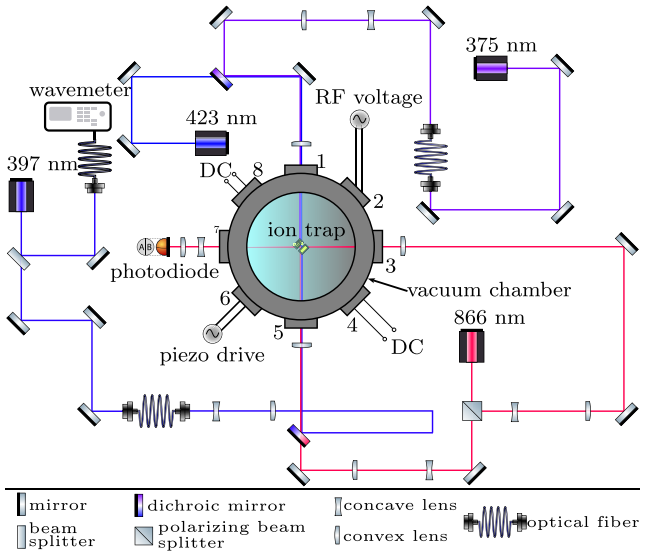

FIG. 2. Schematic of the vacuum chamber and the optical setup. See text for details.

to prevent excessive deposition of metallic calcium on the trap electrodes. The temperature of the oven was maintained at 300–400 °C during operation as monitored by a thermocouple attached to the oven tube. Under these conditions, the build-up of patch potentials on the trap electrodes proved minimal.

Photoionization of ^{40}Ca atoms was achieved using two laser beams at wavelengths 423 and 375 nm overlapping in the trap center.[31] Both laser beams were guided to the experiment via optical fibers, combined on a dichroic mirror and directed at the trap through flange 1 with a series of mirrors. The 423 nm laser excited the $(4s^2)^1S_0 \rightarrow (4s4p)^1P_1$ transition.[32] The subsequent absorption of a 375 nm photon led to the generation of Ca^+ ions to be confined in the trap.

Laser beams at 397 and 866 nm were used for the laser cooling of Ca^+ on the $(4s)^2S_{1/2} \leftrightarrow (4p)^2P_{1/2} \leftrightarrow (3d)^2D_{3/2}$ closed cycling transitions. The beams were combined on a second dichroic mirror and guided through flange 5 to the trap center. The cooling lasers entered the trapping region under an angle of ≈45° with respect to all three principal trapping axes to enable the simultaneous cooling of the trapped ions in all spatial directions. A part of the 866 nm laser beam was separated by a polarizing beam splitter (PBS), inserted into the chamber via flange 3 and used for the optomechanical readout of the nanowire (see Sec. III).

III. METHODS

A. Optical readout of nanowire oscillations

Vibrations and mechanical resonances of the nanowire were characterized inside the experimental chamber using an optical readout.[33,34] The 866 nm laser beam entering the chamber through flange 3 was focused to a beam waist of ≈55 μm onto the nanowire using a lens with focal length f = 200 mm placed outside vacuum. The beam exiting the chamber on the opposing side through flange 7 was recollimated onto a dual-element Si PIN photodiode. The two

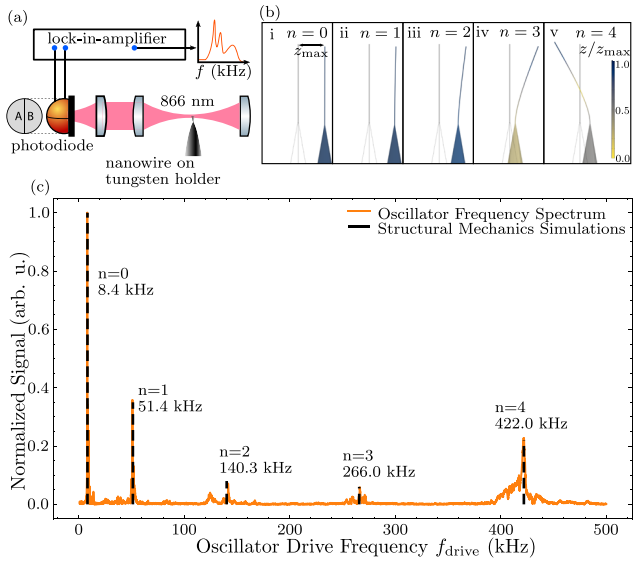

FIG. 3. (a) Optical setup for the readout of the mechanical resonance frequencies of the nanowire assembly. (b) Shapes of the $n = 0$ to $n = 4$ eigenmodes of the nanowire on the conical holder normalized to an arbitrary maximum displacement z_{max} of the nanowire tip obtained from structural mechanics simulations. Empty structures: equilibrium positions. Colored structures: maximum displacements. Darker colors indicate larger displacements, as shown in the color bar. (c) Measured nanowire mechanical excitation spectrum (orange trace) and theoretical frequencies (dashed black lines) of the eigenmodes of the assembly obtained from the numerical simulations.

photodiode segments A, B transmitted a sum $(A + B)$ and a difference $(A - B)$ signal to a lock-in amplifier, as indicated in Fig. 3(a). The mechanically driven nanowire was placed in the focus of the beam, leading to modulations of the signal measured by the photodiode depending on the amplitude of the vibration of the nanowire.

Demodulating the photodiode signal as a function of the drive frequency f_{drive} yielded the mechanical spectrum of the oscillator [orange trace in Fig. 3(c)], showing the resonance frequencies f_n and their assignments to the assembly's mechanical eigenmodes. Figure 3(b) depicts the eigenmodes of the nanowire on its holder as obtained from a structural mechanics simulation using the COMSOL Multiphysics program.[35] The resonance frequencies obtained from the simulations [black dashed lines in Fig. 3(c)] are in good agreement with the experimental results.

B. Measurement of driven ion motion

Driven motion of trapped ions was characterized by time-resolving their periodically changing fluorescence rate using a photon-correlation method. This method is widely used for the determination and minimization of excess micromotion in ion trapping experiments[36,37] but has been applied here for the measurement of the motion of the trapped ions driven by the nanowire. A laser-cooled ion with oscillatory motion at angular frequency ω exhibits a periodic fluorescence rate $R_s(t)$ due to the time-dependent Doppler shift at a detuning $\delta = \delta_0 - kv(t) = \delta_0 - v_{max}\cos(\omega t - \varphi)$ of the cooling laser from the resonance frequency,[36,38]

$$R_s = R_0 \frac{(\Gamma/2)^2}{(\Gamma/2)^2 + (\delta_0 - k v_{max}\cos(\omega t - \varphi))^2}. \quad (1)$$

Here, $k = 2\pi/\lambda$ is the wave number of the cooling laser; Γ is the natural linewidth of the $(4s)^2S_{1/2} \leftrightarrow (4p)^2P_{3/2}$ cooling transition; v_{max} is the amplitude of the oscillating velocity $v(t)$ of the ion; φ is the phase of the motion; δ_0 is the frequency detuning of the cooling laser to the cooling transition in the rest frame; and R_0 is the scattering rate on resonance.

Figure 4(a) schematically shows the experimental setup used for the photon-correlation measurements. Part of the fluorescence of the ions was collected by using a microscope, divided by a 50:50 beam splitter onto a CCD camera for imaging the ions and onto

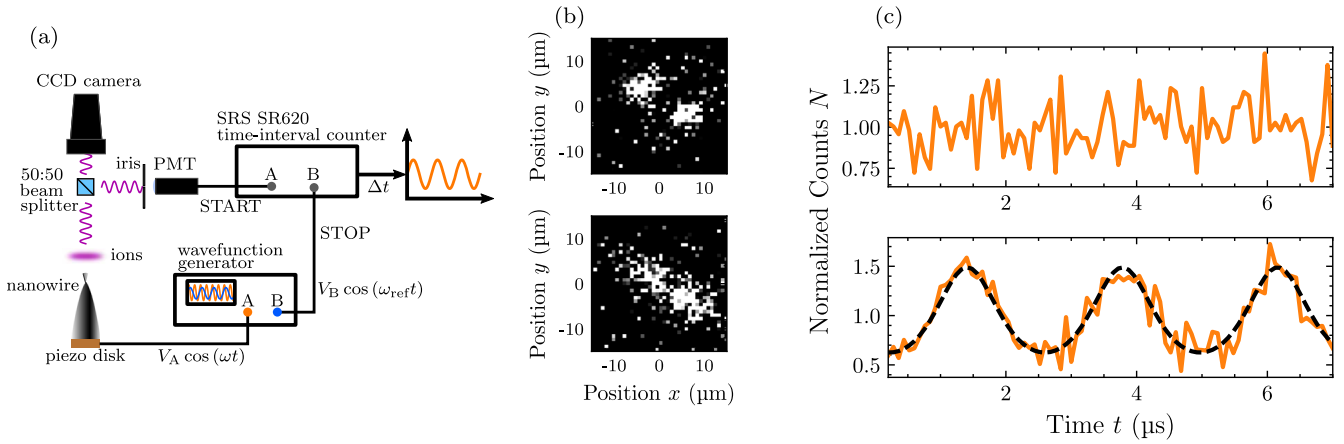

FIG. 4. Characterization of driven ion motion by photon correlation. (a) Schematic of the setup for photon-correlation measurements. See the text for details. (b) CCD camera images of a two-ion string without (top) and with (bottom) drive by the nanowire. (c) Normalized histograms obtained from correlation measurements of the photon counts with the period of the nanowire drive. Undriven ions (top) show no correlation to the reference signal, while resonantly driven ions (bottom) exhibit a periodic fluorescence signal at the drive frequency ω. Dashed line: fit of Eq. (1) to the data.

a photon-multiplier tube (PMT) for the time-resolved correlation measurements. An aperture was positioned in front of the PMT in order to reduce photon counts from spurious light. Detection of a photon by the PMT triggered a time measurement by a universal time-to-amplitude converter (TAC, Stanford Research Systems SR620). The measurement was correlated with a sinusoidal reference signal in order to stop the time measurement whenever the reference signal reached a zero crossing with a negative slope. Typically $N = 10^6$ such time intervals Δt were collected in a measurement. The resulting distribution of time intervals was corrected by a background measurement without drive, normalized by the average number of counts obtained across all time intervals and plotted as histograms with 250 bins, as shown in Fig. 4(c). These time traces revealed the periodic motion of the driven ions in the trap. By setting the reference signal to an integer fraction of the drive signal (here $\omega_{\mathrm{ref}} = \omega/3$), three full periods of the fluorescence rate were

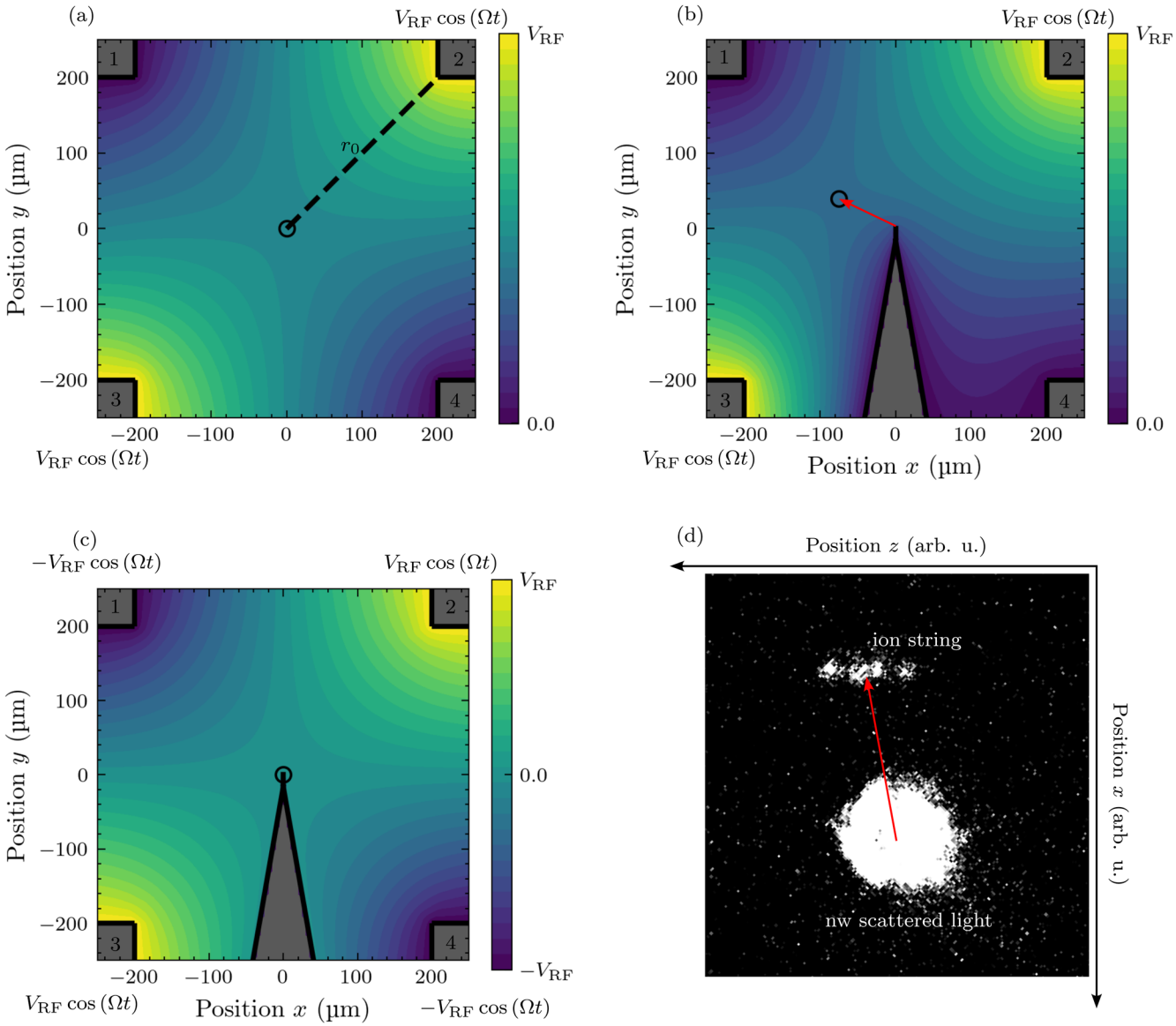

FIG. 5. Numerical RF potentials in the radial plane at $z = 0$. (a) Unperturbed quadrupolar potential generated by a single-phase RF voltage $V_{\mathrm{RF}}\cos(\Omega t)$ applied to electrodes 2 and 3 and electrodes 1 and 4 being kept at electric ground. (b) The introduction of the nanowire close to the trap center leads to a shift of the RF potential saddle point. (c) Operating the trap with voltages $\pm V_{\mathrm{RF}}\cos(\Omega t)$ applied to electrode pairs $(1,4)$ and $(2,3)$ with opposite phases restores symmetry of the RF potential as long as the nanowire is aligned with the y axis. (d) Camera image showing shifts of the ions along x and z due to the introduction of the nanowire close to the trap center. In this position, the ions and the nanowire assembly scatter light from the 397 nm cooling laser. The direction of the shift is consistent with the behavior expected from panel (b).

resolved. The velocity amplitudes v_{max} of the driven ion motions were determined from fits of Eq. (1) to the histograms. For the measurement shown in the bottom panel of Fig. 4, a maximum ion velocity $v_{max} = (47.0 \pm 2.0)$ m/s was determined. To ensure a perfect phase correlation between the driven ion motion and the reference signal, both signals were obtained from the same wavefunction generator, as shown in Fig. 4(a).

IV. CHARACTERIZATION OF NANOWIRE–ION INTERACTION

A. Effect of nanowire on trapping potentials

The main parameters governing the strength of the coupling between the nanowire and trapped ions are the effective charge q_{nw} on the wire and its distance d to the ion. In addition, the excitation of driven ion motion strongly depends on the match of the oscillation frequencies of the two subsystems. We approximate the ion–nanowire interaction potential Φ_{IA} as the one between two point-charges,

$$\Phi_{IA} = k_c \frac{q_{nw} q_{ion}}{\sqrt{(x - x_{nw})^2 + (y - y_{nw})^2 + (z - z_{nw})^2}}. \quad (2)$$

This treatment corresponds to retaining only the leading term in a multipole expansion of the ion–nanowire interaction (see the supplementary material of Ref. 27 for details). Here, (x, y, z) and (x_{nw}, y_{nw}, z_{nw}) are the positions of the ion and the tip of the nanowire, respectively, where the charge is assumed to be localized. k_c is the Coulomb constant, and q_{ion} and q_{nw} are the charges of the ion and nanowire, respectively.

While it is desirable to minimize the ion–nanowire distance d to obtain stronger coupling, the introduction of the nanowire close to the center of the trap leads to significant deviations of the trapping potential from ideal quadrupolar behavior. These deviations are mainly caused by the tungsten holder with diameter $d_{holder} = 250\ \mu$m, which is of comparable size with the individual trap electrode segments. Figure 5 shows cuts through the RF electric potential in the trap in the radial plane without [Fig. 5(a)] and with [Figs. 5(b)] the nanowire present. The potentials were simulated using COMSOL Multiphysics taking into account the realistic geometry of the trap and the nanowire on its holder.

We simulated that operating the trap with RF voltage of a single phase applied to two diagonally opposed electrodes while keeping the remaining electrodes at static potential, as in the present experiments, leading to distortions of the RF potential due to the breaking of the symmetry induced by the tungsten holder. As a result, the saddle point of the RF potential shifts from the geometric trap center. Applying RF voltages of alternating phases to all four electrode stacks restores a higher degree of symmetry to the system as long as the nanowire is centered on the x (or y) axis. In the experiment and without further compensation, the nanowire always shifted the ions from the geometric trap center, as shown in Fig. 5(d). Nonetheless, while the ions may experience excess micromotion[36] in this location, this does not impact the dynamics of their *secular* motion, which can be adiabatically separated. The ions thus experience a locally harmonic effective trapping potential, as assumed in the modeling. However, for future experiments involving cooling of the ions to their motional ground state in the trap, Doppler shifts caused by excess micromotion need to be judiciously minimized for which a symmetric trap-potential configuration such as the one displayed in Fig. 5(c) is more advantageous. For this purpose, a suitable modification of the trap drive allowing more flexible combinations of DC and RF voltages will be implemented.

B. Ion motional frequency shifts

The matching of the axial trap frequency $f_z = \frac{\omega_z}{2\pi}$ to one of the resonance frequencies f_{nw} of the nanowire assembly [Fig. 3(c)] is

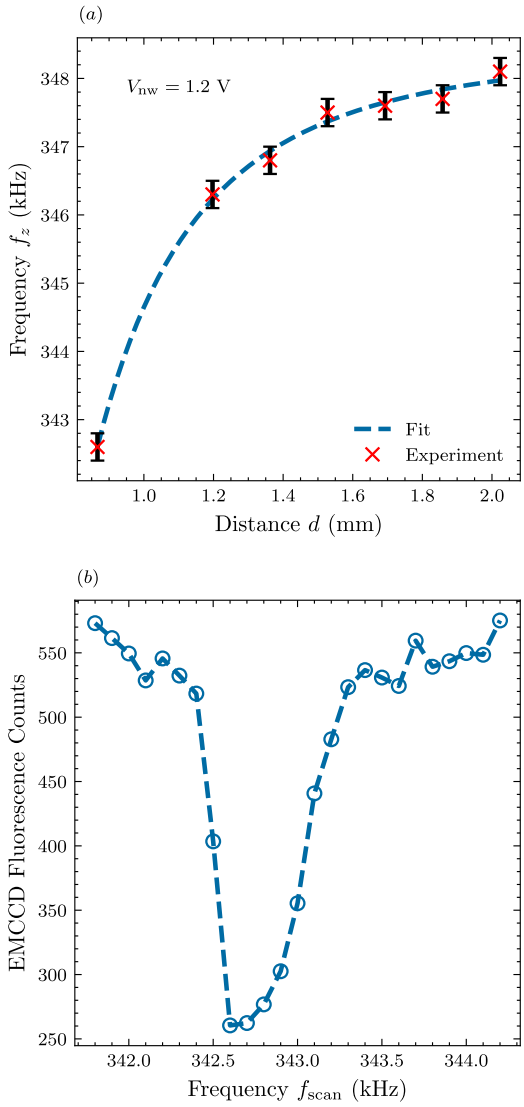

FIG. 6. (a) Ion axial oscillation frequencies f_z for different ion–nanowire distances d at $V_{nw} = 1.2$ V. The dashed line corresponds to a fit of the data to Eq. (3). The frequency converges to $f_0 = 348.4$ kHz for $d \to \infty$ corresponding to the unperturbed oscillation frequency of the ion in the trap. (b) Determination of the axial oscillation frequency of the ions by parametric electrical excitation at $d = 0.87$ mm and $V_{nw} = 1.2$ V. On resonance at $f_z = 342.6 \pm 0.2$ kHz, the fluorescence yield of the ions is decreased due to their motional excitation.

crucial for efficient energy transfer between the two systems. Variations of coupling parameters such as the ion–nanowire distance d and the effective nanowire charge q_{nw} result in shifts of the effective trapping frequency f_z experienced by the ions due to the change in potential. This requires the adjustment of the trapping potential using voltages applied to the DC electrodes to preserve the resonance condition $f_z = f_{nw}$. Assuming a harmonic trapping potential $\Phi_{trap} = \frac{1}{2} m\omega_{trap}^2 z^2$, the expected change in frequency $\omega_{trap} \to \omega_z$ due to Eq. (2) can be approximated by a Taylor expansion,[39]

$$\omega_z = \sqrt{\omega_{trap}^2 - \frac{\varepsilon}{md^3} + \frac{3\varepsilon z_{nw}^2}{md^5}}. \quad (3)$$

Here, we defined the parameter $\varepsilon = k_c q_{ion} q_{nw}$, which is proportional to the static voltage V_{nw} applied to the nanowire. Thus, the frequency change given by Eq. (3) mainly depends on the ion–nanowire distance d and the effective charge q_{nw} on the nanowire. Figure 6(a) shows the experimentally obtained axial frequency shifts for a variation of d at $V_{nw} = 1.2$ V. The nanowire was positioned below the trapped ions along the vertical y axis at $(x_{nw}, y_{nw}, z_{nw}) = (0, -d, 0)$, i.e., $z_{nw} = 0$ in Eq. (3). The ion–nanowire distance d was large enough such that no shifts of the ion equilibrium positions were observable. The step size of the nanopositioners was determined from a fit of Eq. (3) to the experimental data to be 330 nm/step. The resulting axial frequencies f_z were measured by parametric electrical excitation[40] of the ion motion, as shown in Fig. 6(b).

C. Mechanical excitation of ions

The $n = 4, f_{nw} = 422$ kHz mechanical resonance of the nanowire assembly [Fig. 3(c)] was chosen for the mechanical excitation of the trapped ions because stable trapping conditions for the ions can readily be achieved at this trap frequency. Single ions or strings of few ions were loaded into the trap and the axial trap frequency was adjusted to $f_z = (422 \pm 0.2)$ kHz to obtain resonance with the mechanical oscillator. Applying a mechanical drive to the nanowire then also leads to a visible excitation of the ion motion in the camera images, as shown in Fig. 4(b): the initially well-localized undriven ions [Fig. 4(b), top] were resonantly driven by the mechanical motion of the nanowire. The image captured by the EMCCD camera showed a delocalization of the ion positions along the longitudinal direction due to their large-amplitude oscillation induced by the nanowire [Fig. 4(b), bottom]. In this experiment, a static voltage $V_{nw} = 1.2$ V was applied to the nanowire and its tip was positioned at an ion–nanowire distance of around $d \approx 300\ \mu$m.

V. CONCLUSION AND OUTLOOK

In this article, we described in detail the experimental implementation of a novel hybrid system consisting of Ca^+ ions confined in a linear radio frequency trap combined with an Ag_2Ga nano-oscillator. The system was designed to couple its constituents via their mutual Coulomb interaction and resonantly address the ion motion with the mechanical drive of the nano-oscillator. Introduction of the nanowire to the ion trap region leads to distortions from the ideal trapping potential of a linear trap. The resulting frequency shifts were experimentally confirmed for a variety of ion-nanowire positions, d, consistent with the expectations from a theoretical model. We also characterized in detail the interaction of the ion with the nanowire and the resonant motional excitation of the ions by the mechanical drive in the classical regime.

The presented characterization and demonstration of the ion-nanowire system shows the possibility of coupling to and mechanically driving the trapped ion motion. Future experiments will extend control over the system to manipulate ultracold trapped ion motional states on the quantum level.[26]

ACKNOWLEDGMENTS

We thank Dr. Anatoly Johnson, Georg Holderied, Philipp Knöpfel, and Grischa Martin for providing technical assistance. We thank Dr. Adrien Poindron for useful discussions. This work was supported by the Swiss Nanoscience Institute (Grant No. P1808), the Swiss National Science Foundation (Grant No. 200021 204123), and the University of Basel.

AUTHOR DECLARATIONS

Conflict of Interest

The authors have no conflicts to disclose.

Author Contributions

M. Weegen: Formal analysis (equal); Investigation (equal); Methodology (equal); Software (equal); Visualization (equal); Writing – original draft (equal); Writing – review & editing (equal). **P. N. Fountas**: Investigation (equal); Methodology (equal); Software (equal); Writing – review & editing (equal). **M. Poggio**: Conceptualization (equal); Funding acquisition (equal); Investigation (equal); Methodology (equal); Project administration (equal); Resources (equal); Supervision (equal); Validation (equal); Writing – original draft (equal); Writing – review & editing (equal). **S. Willitsch**: Conceptualization (equal); Funding acquisition (equal); Investigation (equal); Methodology (equal); Project administration (equal); Resources (equal); Supervision (equal); Validation (equal); Writing – original draft (equal); Writing – review & editing (equal).

DATA AVAILABILITY

The data that support the findings of this study are openly available in Xenodo at http://doi.org/10.5281/zenodo.14729559, DOI: 10.5281/zenodo.14729559.

REFERENCES

[1] M. Wallquist, K. Hammerer, P. Rabl, M. Lukin, and P. Zoller, "Hybrid quantum devices and quantum engineering," Phys. Scr. **2009**(T137), 014001.
[2] P. Treutlein, C. Genes, K. Hammerer, M. Poggio, and P. Rabl, "Hybrid mechanical systems," in *Cavity Optomechanics*, edited by M. Aspelmeyer, T. J. Kippenberg, and F. Marquardt (Springer, Berlin, Heidelberg, 2014), p. 327.
[3] S. Kotler, R. W. Simmonds, D. Leibfried, and D. J. Wineland, "Hybrid quantum systems with trapped charged particles," Phys. Rev. A **95**, 022327 (2017).
[4] G. Kurizki, P. Bertet, Y. Kubo, and J. Schmiedmayer, "Quantum technologies with hybrid systems," PNAS **112**, 3866 (2015).
[5] L. Tian and P. Zoller, "Coupled ion-nanomechanical systems," Phys. Rev. Lett. **93**, 266403 (2004).

[6]K. Hammerer, M. Aspelmeyer, E. S. Polzik, and P. Zoller, "Establishing Einstein-Poldosky-Rosen channels between nanomechanics and atomic ensembles," Phys. Rev. Lett. **102**, 020501 (2009).
[7]D. Hunger, S. Camerer, M. Korppi, A. Jöckel, T. W. Hänsch, and P. Treutlein, "Coupling ultracold atoms to mechanical oscillators," C. R. Phys. **12**, 871 (2011).
[8]A. A. Geraci and J. Kitching, "Ultracold mechanical resonators coupled to atoms in an optical lattice," Phys. Rev. A **80**, 032317 (2009).
[9]H. Wang and I. Lekavicius, "Coupling spins to nanomechanical resonators: Toward quantum spin-mechanics," Appl. Phys. Lett. **117**, 230501 (2020).
[10]J. Clarke and F. K. Wilhelm, "Superconducting quantum bits," Nature **453**, 1031 (2008).
[11]Z.-L. Xiang, S. Ashhab, J. Q. You, and F. Nori, "Hybrid quantum circuits: Superconducting circuits interacting with other quantum systems," Rev. Mod. Phys. **85**, 623 (2013).
[12]F. J. Giessibl, "Advances in atomic force microscopy," Rev. Mod. Phys. **75**, 949 (2003).
[13]A. Bachtold, J. Moser, and M. I. Dykman, "Mesoscopic physics of nanomechanical systems," Rev. Mod. Phys. **94**, 045005 (2022).
[14]F. G. Major, V. N. Gheorghe, and G. Werth, *Charged Particle Traps* (Springer, Berlin and Heidelberg, 2005).
[15]D. Leibfried, R. Blatt, C. Monroe, and D. Wineland, "Quantum dynamics of single trapped ions," Rev. Mod. Phys. **75**, 281 (2003).
[16]H. Häffner, C. F. Roos, and R. Blatt, "Quantum computing with trapped ions," Phys. Rep. **469**, 155 (2008).
[17]K. R. Brown, C. Ospelkaus, Y. Colombe, A. C. Wilson, D. Leibfried, and D. J. Wineland, "Coupled quantized mechanical oscillators," Nature **471**, 196 (2011).
[18]M. Harlander, R. Lechner, M. Brownnutt, R. Blatt, and W. Hänsel, "Trapped-ion antennae for the transmission of quantum information," Nature **471**, 200 (2011).
[19]M. Poggio, C. L. Degen, H. J. Mamin, and D. Rugar, "Feedback cooling of a cantilever's fundamental mode below 5 mK," Phys. Rev. Lett. **99**, 017201 (2007).
[20]J. Chan, T. P. Mayer Alegre, A. H. Sfavi-Naeini, J. T. Hill, A. Krause, S. Gröblacher, M. Aspelmeyer, and O. Painter, "Laser cooling of a nanomechanical oscillator into its quantum ground state," Nature **478**, 89 (2011).
[21]A. Jöckel, A. Faber, T. Kampschulte, M. Korppi, M. T. Rakher, and P. Treutlein, "Sympathetic cooling of a membrane oscillator in a hybrid mechanical-atomic system," Nat. Nanotech. **10**, 55 (2015).
[22]G.-L. Schmid, C. T. Ngai, M. Ernzer, M. B. Aguilera, T. M. Karg, and P. Treutlein, "Coherent feedback cooling of a nanomechanical membrane with atomic spins," Phys. Rev. X **12**, 011020 (2022).
[23]D. J. Wineland, C. Monroe, W. M. Itano, D. Leibfried, B. E. King, and D. M. Meekhof, "Experimental issues in coherent quantum-state manipulation of trapped atomic ions," J. Res. Natl. Inst. Stand. Technol. **103**, 259 (1998).
[24]S. C. Burd, R. Srinivas, J. J. Bollinger, A. C. Wilson, D. J. Wineland, D. Leibfried, D. H. Slichter, and D. T. C. Allcock, "Quantum amplification of mechanical oscillator motion," Science **364**, 1163 (2019).
[25]M. J. Biercuk, H. Uys, J. W. Britton, A. P. VanDevender, and J. J. Bollinger, "Ultrasensitive detection of force and displacement using trapped ions," Nat. Nanotechnol. **5**, 646 (2010).
[26]P. N. Fountas, M. Poggio, and S. Willitsch, "Classical and quantum dynamics of a trapped ion coupled to a charged nanowire," New J. Phys. **21**, 013030 (2019).
[27]M. Weegen, M. Poggio, and S. Willitsch, "Coupling trapped ions to a nanomechanical oscillator," Phys. Rev. Lett. **133**, 223201 (2024).
[28]J. D. Siverns, S. Weidt, K. Lake, B. Lekitsch, M. D. Hughes, and W. K. Hensinger, "Optimization of two-dimensional ion trap arrays for quantum simulation," New J. Phys. **14**, 085009 (2012).
[29]M. Drewsen, A. Mortensen, R. Martinussen, P. Staanum, and J. L. Sørensen, "Nondestructive identification of cold and extremely localized single molecular ions," Phys. Rev. Lett. **93**, 243201 (2004).
[30]L. B. Biedermann, R. C. Tung, A. Raman, R. G. Reifenberger, M. M. Yazdanpanah, and R. W. Cohn, "Characterization of silver–gallium nanowires for force and mass sensing applications," Nanotechnology **21**, 305701 (2010).
[31]D. M. Lucas, A. Ramos, J. P. Home, M. J. McDonnell, S. Nakayama, J.-P. Stacey, S. C. Webster, D. N. Stacey, and A. M. Steane, "Isotope-selective photoionization for calcium ion trapping," Phys. Rev. A **69**, 012711 (2004).
[32]E. J. Salumbides, V. Maslinskas, I. M. Dildar, A. L. Wolf, E. J. van Duijn, K. S. E. Eikema, and W. Ubachs, "High-precision frequency measurement of the 423-nm Ca i line," Phys. Rev. A **83**, 012502 (2011).
[33]B. Sanii and P. D. Ashby, "High sensitivity deflection detection of nanowires," Phys. Rev. Lett. **104**, 147203 (2010).
[34]A. Gloppe, P. Verlot, E. Dupont-Ferrier, A. Siria, P. Poncharal, G. Bachelier, P. Vincent, and O. Arcizet, "Bidimensional nano-optomechanics and topological backaction in a non-conservative radiation force field," Nat. Nanotechnol. **9**, 920 (2014).
[35]COMSOL (Comsol Multiphysics, Stockholm, Sweden, 2024), Vol. 6.2.
[36]D. J. Berkeland, J. D. Miller, J. C. Bergquist, W. M. Itano, and D. J. Wineland, "Minimization of ion micromotion in a Paul trap," J. Appl. Phys. **83**, 5025 (1998).
[37]J. Keller, H. L. Partner, T. Burgermeister, and T. E. Mehlstäubler, "Precise determination of micromotion for trapped-ion optical clocks," J. Appl. Phys. **118**, 104501 (2015).
[38]B. Wang, J. W. Zhang, Z. H. Lu, and L. J. Wang, "Direct measurement of micromotion speed in a linear quadrupole trap," J. Appl. Phys. **108**, 013108 (2010).
[39]M. Weegen, Mechanical Excitation of Trapped Ions Coupled to a Nanomechanical Oscillator, Ph.D. thesis, University of Basel, 2024.
[40]X. Zhao, V. L. Ryjkov, and H. A. Schuessler, "Parametric excitations of trapped ions in a linear rf ion trap," Phys. Rev. A **66**, 063414 (2002).